

Comparisons of forecasting for hepatitis in Guangxi province, China by using three neural networks models

Ruijing Gan¹, Ni Chen¹, Daizheng Huang^{Corresp. 1}

¹ School of Preclinical Medicine, Guangxi Medical University, Nanning, Guangxi, China

Corresponding Author: Daizheng Huang

Email address: daizheng-huang@qq.com

This study compares and evaluates the prediction of hepatitis in Guangxi Province, China by using back propagation neural networks based genetic algorithm (BPNN-GA), generalized regression neural networks (GRNN), and wavelet neural networks (WNN). In order to compare the results of forecasting, the data obtained from 2004 to 2013 and 2014 were used as modeling and forecasting samples, respectively. The results show that when the small data set of hepatitis has seasonal fluctuation, the prediction result by BPNN-GA will be better than the two other methods. The WNN method is suitable for predicting the large data set of hepatitis that has seasonal fluctuation and the same for the GRNN method when the data increases steadily.

1 **Comparisons of Forecasting for Hepatitis in Guangxi Province,**

2 **China by Three Neural Network Models**

3 Ruijing Gan, Ni Chen, Daizheng Huang*

4 School of Preclinical Medicine, Guangxi Medical University, China

5 *Corresponding author: daizheng-huang@qq.com

6 **Abstract:** This study compares and evaluates the prediction of hepatitis in Guangxi
7 Province, China by using back propagation neural networks based genetic algorithm (BPNN-
8 GA), generalized regression neural networks (GRNN), and wavelet neural networks (WNN). In
9 order to compare the results of forecasting, the data obtained from 2004 to 2013 and 2014 were
10 used as modeling and forecasting samples, respectively. The results show that when the small
11 data set of hepatitis has seasonal fluctuation, the prediction result by BPNN-GA will be better
12 than the two other methods. The WNN method is suitable for predicting the large data set of
13 hepatitis that has seasonal fluctuation and the same for the GRNN method when the data
14 increases steadily.

15 **Key words:** hepatitis; forecasting; neural networks method; evaluation

16 **Introduction**

17 Hepatitis, which is an inflammation of the liver caused by a virus, is categorized into five
18 different types: hepatitis A, B, C, D, and E. All of these viruses cause short term or acute
19 infection; however, the hepatitis B, C, and D viruses can cause a long-term infection, called
20 chronic hepatitis, which can lead to life-threatening complications such as cirrhosis (liver

21 scarring), liver failure, and liver cancer (1). Hepatitis causes an enormous amount of human
22 suffering, particularly in Asia, sub-Saharan Africa, parts of the Arabian Peninsula, the South
23 Pacific, tropical South America, and Arctic North America (2). Viral hepatitis kills 1.5 million
24 people every year and over one-third of the world's population (more than 2 billion people)
25 have been or are actively infected by the hepatitis B virus (HBV) (1, 3). It has been reported
26 that the direct costs due to hepatitis B reach around 500 MM Yuan RMB (approximately 80MM
27 US dollar) in China every year (4). Guangxi, officially known as Guangxi Zhuang Autonomous
28 Region (GZAR), is a Chinese autonomous region in South Central China that is located in the
29 southern part of the country and is bordered to Vietnam in the southwest and the Gulf of Tonkin
30 in the south ($20^{\circ}54'26''$ N, $104^{\circ}26' - 112^{\circ}04'$ E). It occupies an area of 236,700 km² with a
31 population of over 47 million people in 2014. The typical year-round climate is subtropical
32 rainy, which consists of long, hot summers and short winters. The annual mean temperature and
33 rainfall are 16°C to 23°C and 1080 mm to 2760 mm, respectively (5). Guangxi Province is a
34 high-incidence area of viral hepatitis. Hepatitis B has been in the top three infectious diseases in
35 Guangxi Province for the past ten years. Therefore, accurate incidence forecasting of hepatitis is
36 critical for early prevention and for better strategic planning by the government.

37 Prediction of incidences of hepatitis diseases has been an ongoing effort and several
38 complex statistical models have been offered. Zhang proposed a Nash nonlinear grey Bernoulli
39 model termed PSO-NNGBM (1,1) to forecast the incidence of hepatitis B in Xinjiang,
40 China(6). Ren proposed a combined mathematical model using an autoregressive integrated
41 moving average model (ARIMA) and a back propagation neural network (BPNN) to forecast

42 the incidence of hepatitis E in Shanghai, China (7). Ture compared time series prediction
43 capabilities of three artificial neural networks (ANN), algorithms (multi-layer perceptron
44 (MLP), radial basis function (RBF), time delay neural networks (TDNN)), and an auto-
45 regressive integrated moving average (ARIMA) model to HAV forecasting (8). Gan used a
46 hybrid algorithm combining grey model and back propagation artificial neural network to
47 forecast hepatitis B in China (9). A mathematical model of HBV transmission was used to
48 predict future chronic hepatitis B (CHB) prevalence in the New Zealand Tongan population
49 with different infection control strategies in literature (10). Other studies have been performed
50 with supervised methods for predicting viruses and pathologies (11, 12, 13).

51 We note that nonlinear relationships may exist among the monthly incidences of hepatitis.
52 While the ARIMA model can only extract linear relationships within the time series data and
53 does not efficiently extract the full relationship hidden in the historical data. The artificial
54 neural network (ANN) time series models can capture the historical information by nonlinear
55 functions (5).

56 An artificial neural network employs nonlinear mathematical models to mimic the human
57 problem-solving process by learning previously observations to build a system of "neurons"
58 that makes new decisions, classifications, and forecasts (14, 15). The ANN model has been
59 successfully used to predict hepatitis A (16).

60 The aim of this study was to use three neural networks methods, namely, back propagation
61 neural networks based on genetic algorithm (BPNN-GA), wavelet neural networks (WNN), and
62 generalized regression neural networks (GRNN) to forecast hepatitis in the Guangxi Province
63 of China, and compare the performance of these three methods. This comparison may be

64 helpful for epidemiologists in choosing the most suitable methodology in a given situation.

65 **Materials and Methods**

66 **Materials**

67 The incidence of hepatitis data, including hepatitis A, B, C, and E, were collected on a
68 monthly base from the Chinese National Surveillance System (17) and the Guangxi Health
69 Information Network (18) from January 2004 to December 2014. These data composed the time

70 series $X = \{x(0), x(1), \dots, x(131)\}$. The information belongs to the government statistical data and is
71 available to the public. Hepatitis D has not been considered because the data cannot be obtained
72 from the Chinese National Surveillance System and the Guangxi Health Information Network.
73 The incidence dataset between 2004 and 2013 was used as the training sample to fit the model,
74 and the dataset in 2014 was used as the testing sample.

75 **Methods**

76 Three artificial neural networks methods: BPNN-GA, WNN, and GRNN, were used for
77 prediction and their performances were compared.

78 **BPNN-GA Model**

79 BPNN is a multi-layered feed-forward neural network; the main features are that the signal
80 transports forward, and the error transports backward. The input signal will be processed layer-
81 by-layer from the input layer to the output layer. The next state of the neuron is only affected by
82 the front state of the neuron in the layer. If the expected output was not received, the weights
83 and the thresholds of the network will be adjusted by the error that transports backward.

84 Therefore, the desired output will be achieved in an iterative manner (19).

85 If the model of BPNN has i input nodes, j hidden nodes, and k output nodes, there will be
86 weight variables of dimensionality $N = i \times j$ between the input layer and the hidden layer, $j \times 1$
87 threshold variables in hidden layer, weight variable of dimensionality $M = j \times k$ between the
88 hidden layer and the output layer, and $k \times 1$ threshold variables in the output layer (20). The
89 topology structure is shown in Figure 1.

90 **Figure 1** Topology structure of BPNN.

91 GA is a search heuristic that mimics the process of natural selection. This heuristic is
92 routinely used to generate useful solutions to optimization and search problems (21). The initial
93 weights and thresholds of BPNN are optimized by GA, which is called the BPNN-GA method.
94 The algorithm of the BPNN-GA flow chart is shown in Figure 2.

95 **Figure 2** Flow chart of the BPNN prediction algorithm optimized by GA.

96 **WNN model**

97 WNN is a kind of neural network with a structure that is established on the basis of BPNN,
98 and the wavelet basis function is taken as the transfer function is in hidden layer nodes. The
99 signal also transports forward and the error transports backward. The topology structure is
100 shown in Figure 3. WNN includes two new variables, a scale factor, a displacement factor,
101 which give it excellent functional approximation. The WNN method is composed of relatively
102 less expensive terms that often has fast functional approximation abilities and good predicting
103 precision (due to its ability to sift out the parameters). Compared to BPNN, the weight
104 coefficient of WNN has the characteristics of linearity, and the objective function of learning
105 has the feature of convexity. These properties will avoid being nonlinear in local optimization

106 | when the network is trained (22, 23).

107 | **Figure 3** Topology structure of WNN.

108 | The formula for calculating the hidden layer for an input signal sequence is

109 $x_i(i=1,2,\dots,k)$ is as follows:

$$110 \quad h(j) = h_j \left[\frac{\sum_{i=1}^k \omega_{ij} x_i - b_j}{a_j} \right] \quad j=1,2,\dots,l$$

111 where k is the number of input signal; l is the number of nodes in the hidden layer; $h(j)$ is

112 the output of the j th node in the hidden layer; h_j is the wavelet basis function; ω_{ij} is the

113 weights between the input layer and hidden layer; a_j is the scale factor of h_j and b_j

114 is the displacement factor of h_j .

115 The formula to calculate the output layer is as follows.

$$116 \quad y(k) = \sum_{i=1}^l \omega_{ik} h(i) \quad k=1,2,\dots,m$$

117 where $h(i)$ is the output of the i th node in the hidden layer; l is the number of nodes in the

118 hidden layer; m is the number of nodes in the output layer; and ω_{ij} is the weight between the
 119 hidden layer and the output layer.

120 The weights of the network, the scale factor, and the displacement factor were estimated by
 121 the steepest descent method in WNN. The correction process of prediction used by WNN
 122 follows.

123 **Step 1.** Calculate error of prediction.

$$124 \quad e = \sum_{k=1}^m yn(k) - y(k)$$

125 where $yn(k)$ is the expected output, namely the true value. $y(k)$ is the forecasting
 126 output.

127 **Step 2.** Correct the weight of the network and the coefficients of wavelet basis function
 128 according to the prediction error.

$$129 \quad \omega_{n,k}^{(i+1)} = \omega_{n,k}^i + \Delta\omega_{n,k}^{(i+1)}$$

$$130 \quad a_k^{(i+1)} = a_k^i + \Delta a_k^{(i+1)}$$

$$131 \quad b_k^{(i+1)} = b_k^i + \Delta b_k^{(i+1)}$$

132 where

$$133 \quad \Delta\omega_{n,k}^{(i+1)} = -\eta \frac{\partial e}{\partial \omega_{n,k}^{(i)}}$$

134
$$\Delta a_k^{(i+1)} = -\eta \frac{\partial e}{\partial a_k^{(i)}}$$

135
$$\Delta b_k^{(i+1)} = -\eta \frac{\partial e}{\partial b_k^{(i)}}$$

136 and η is the learning rate.

137 The algorithm of WNN flow chart is shown in Figure 4.

138 **Figure 4** Flow chart of the WNN prediction algorithm.

139 GRNN Model

140 GRNN is a memory-based network that provides estimates of continuous variables and
141 converges to the underlying (linear or nonlinear) regression surface (24). One advantage of it is
142 the simplicity. The adjustment of one parameter, namely, the spreading factor, is sufficient for
143 determining the network.

144 The topology structure of GRNN consists of four layers: the input layer, the pattern layer,
145 the summation layer, and the output layer. The topology structure is shown in Figure 5.

146 **Figure 5** Topology structure of GRNN.

147 The number of neurons in the input layer is equal to the dimension of the input vector of
148 the learning samples. Every neuron in the input layer is the simple distribution unit and directly
149 transmits the input variables to the pattern layer.

150 The neurons in the pattern layer and the neurons in the input layer have the same number
151 and every one of the neurons in the pattern layer corresponds to a different sample. The transfer
152 function of neurons in the pattern layer is as follows

$$153 \quad \begin{array}{c} X - X_i \\ \vdots \\ \vdots \\ -\vdots \\ P_i = e^{\vdots} \end{array} \begin{array}{l} \sigma^T (X - X_i) \\ \\ \\ \\ \end{array} \quad i=1,2,\dots,n$$

154 where P_i is the output of neurons in the pattern layer; $X = [x_1, x_2, \dots, x_n]^T$ is the input
 155 vector; X_i is the learning samples of the i -th neurons; n is the number of input; i
 156 is the number of neurons; and σ is the smoothness factor.

157 There are two kinds of summation for the neurons in the summation layer. The first one is
 158 that the arithmetic sum is calculated for the output of neurons in the pattern layer. The weight
 159 between the pattern layer and every neuron is 1. The transfer function is shown in formula as
 160 follows.

$$161 \quad \begin{array}{c} X - X_i \\ \vdots \\ \vdots \\ -\vdots \\ P_i = e^{\vdots} \end{array} \begin{array}{l} \sigma^T (X - X_i) \\ \\ \\ \\ \end{array} \quad i=1,2,\dots,n$$

$$S_D = \sum_{i=1}^n P_i = \sum_{i=1}^n \square e^{\vdots}$$

162 The second one is the weighted sum performed for the output of neurons in the pattern
 163 layer. The weight between the i -th neuron in the pattern layer and the j -th summation neuron is

164 equal to the j -th element in the i -th output samples of Y_i . The transfer function is given
 165 below:

$$S_{Nj} = \sum_{i=1}^n Y_{ij} P_i = \sum_{i=1}^n Y_i e^{\zeta_j^T (X - X_i)} \quad j=1,2,\dots,k$$

167 where k is the dimension of the output vector.

168 The number of neurons in the output layer is equal to the dimension of the input vector of
 169 the learning samples. The output of the j -th neurons is shown in formula as follows.

$$y_j = \frac{S_{Nj}}{S_D} \quad j=1,2,\dots,k$$

171 Results

172 The incidence of hepatitis that took place in Guangxi Province from January 2004 to
 173 November 2014 is considered as the original time series $X = \{x(0), x(1), \dots, x(131)\}$ and is shown
 174 in Figure 6.

175 **Figure 6** The main incidence of hepatitis in Guangxi Province, China from January 2004 to
 176 December 2014.

177 The incidence dataset between 2004 and 2013 was used as the training sample to fit the

178 model, and the dataset in 2014 was used as the testing sample.

179 Of all three types of ANN, the optimal four layer neurons were experimentally selected and
180 have average square error less than 0.01. The output layer only contains one neuron
181 representing the forecast value of the incidence of the next month.

182 The hidden node n_2 and the input node n_1 in the three-layer BPNN-GA were related by $n_2 =$
183 $2n_1 + 1$ and a three-layer BPNN-GA model with 4 input nodes, 9 hidden nodes, and 1 output
184 node (4-9-1) was obtained. The selection for parameters of BPNN and GA are based on the
185 literature (25) and (26), respectively. S-tangent function $\text{tansig}()$ and S-log function $\text{logsig}()$
186 were used as transfer functions of the hidden layer neurons and the output layer neurons,
187 respectively. The error between the training output and the expected output (actual output) was
188 0.001, learning rate was 0.9, momentum factor was 0.95, the training time was 1000 iterations,
189 and the parameters of GA were as shown in Table 1.

190 **Table 1** Parameters of the GA used to optimize the BPNN.

191 There were 4 input nodes, 6 hidden nodes, and 1 output node in (4-6-1) WNN. The weights
192 of the network, the scale factor, and the displacement factor were estimated by the steepest
193 descent method. The initial weight was 0.01, learning rate of parameter was 0.001, and the
194 number of iterative learning was 100. The mother wavelet basis function of Morlet was used in
195 the paper which is shown as follows.

196
$$y = \cos(1.75x) e^{-x^2/2}$$

197 4-fold cross validation was experimentally selected and has the best prediction, which is
198 employed to train the GRNN model and the optimal spreading factor was calculated by looping

199 from 0.1 to 2 intervals 0.1. The transfer function of the summation layer neurons used in the
 200 paper is shown as follows.

$$201 \quad S_D = \sum_{i=1}^n P_i = \sum_{i=1}^n \frac{X - X_i \cdot \frac{e^{\frac{X - X_i}{\sigma}}}{1 + e^{\frac{X - X_i}{\sigma}}}}{1 + e^{\frac{X - X_i}{\sigma}}} \quad i=1,2,\dots,n$$

202 where P_i is the output of the pattern layer neurons; $X = [x_1, x_2, \dots, x_n]^T$ is the input
 203 vector; X_i is the learning samples of the i -th neurons; n is the number of input; i is
 204 the number of neurons; and σ is the smoothness factor.

205 The contrast between the observed values and the predicted values obtained through the
 206 three methods are shown in Figure 7.

207 **Figure 7** Contrast between observed values and predicted values using the three methods.

208 Discussion

209 The Relationship Between Predictions and Seasonal Fluctuation Index

210 The seasonal fluctuation index of incidence is used to reveal the fluctuations of incidence
 211 with seasons. The seasonal fluctuation index of the same month in eleven years from 2004 to
 212 2014 can be calculated as:

213
$$SFI1 = \frac{|\bar{x}_{\text{same}} - \bar{x}_{\text{all}}|}{\bar{x}_{\text{all}}}$$

214 where \bar{x}_{same} is the average incidence of the same month and \bar{x}_{all} is the average incidence
215 of all of the months from 2004 to 2014.

216 The seasonal fluctuation index of the every month in 2014 is calculated as:

217
$$SFI2 = \frac{|x_i - \bar{x}|}{\bar{x}}, i = 1, \dots, 12$$

218 where x is the incidence in each month and \bar{x} is the average incidences of all of the
219 months in 2014.

220 Obviously, the greater the number that the seasonal fluctuation index is, the more
221 seasonal volatility of incidence is. That is to say, the index changes reflect the disease
222 variation in the different months. In order to compare the relationship between the seasonal
223 fluctuation index of incidence and the three prediction results, the relative error of prediction
224 is defined as:

225
$$RE_i = \frac{|\hat{y}_i - y_i|}{y_i}, i = 1, 2, \dots, n$$

226 where \hat{y}_i is the predicted value and y_i are the observed values.

227 The seasonal fluctuation index of incidence and the relative error of the three prediction
228 results are shown in Figure 8.

229 **Figure 8.** The relationship between the seasonal fluctuation index and RE of the predictions by
230 the three methods. (Histograms and curves represent RE of the predictions and the seasonal
231 fluctuation index, respectively)

232 Looking at Figure 8, it can be seen that: 1) hepatitis A, B, and E have obvious seasonal
233 characteristics. For Hepatitis B, in particular, the incidence which happens annually in
234 January and February is relatively high with a rapid decline in March. April to September is
235 relatively stable, but from October to December it began to rise significantly; 2) the greater
236 the seasonal fluctuation index of the every month in 2014, the greater the relative error,
237 especially in hepatitis C and E, which shows that the greater the disease fluctuations, the
238 worse the prediction results; 3) the absolute error of the BPNN-GA is smaller than that of the
239 other two methods when the incidence data is stable, such as from April to August for
240 hepatitis A; the absolute error of the GRNN is smaller than that of the other two methods
241 when the incidence data has great fluctuation, such as March, July, and December for
242 hepatitis C and August, October, November, and December for in hepatitis E; and 4) the
243 absolute error of the GRNN is larger than that of the other two methods when the incidence
244 data is larger, and the absolute error of the WNN is larger than that of the other two methods
245 when the incidence data is smaller. The size relationship of the average incidence is: $B > C > E$
246 $> A$. When the incidence data is large, such as the data for hepatitis B, the size relationship of
247 the absolute error of three methods is: $GRNN > BPNN-GA > WNN$.

248 **Comparison of Evaluation Indexes**

249 The mean square error (MSE), root mean square error (RMSE), mean average error
250 (MAE), mean average percentage error (MAPE), and sum of squared error (SSE), have been

251 calculated and compared with the three methods. The performance indexes are defined as
252 shown in the following.

253
$$MSE = \frac{1}{n} \sum_{i=1}^n (\hat{y}_i - y_i)^2$$

254
$$MAE = \frac{1}{n} \sum_{i=1}^n |\hat{y}_i - y_i|$$

255
$$RMSE = \sqrt{\frac{1}{n} \sum_{i=1}^n (\hat{y}_i - y_i)^2}$$

256
$$MAPE = \frac{1}{n} \sum_{i=1}^n |\hat{y}_i - y_i| * 100$$

257
$$SSE = \sum_{i=1}^n (\hat{y}_i - y_i)^2$$

258 where \hat{y}_i is the predicted value and y_i are the observed value.

259 The main evaluation indexes that were calculated by these three methods are listed in Table
260 2.

261 **Table 2** Comparison of the evaluation indexes in the prediction results.

262 (best performers are in bold fonts)

263 From the definitions of the other evaluation indexes, including MSE, MAE, RMSE, SSE,
264 and MAPE, we know that the smaller the values of these indexes are, the more accurate the
265 prediction is. The BPNN-GA method had the smallest values of these evaluation indexes when
266 it was used to predict hepatitis A and the WNN method had the smallest values of these indexes
267 when it was used to predict hepatitis B; the same for the GRNN method when it was used to
268 predict hepatitis E. It can be seen that the BPNN-GA and WNN methods were not superior to
269 the others when they were used to predict hepatitis C, but they were all superior to GRNN
270 method. According to Figure 8, we know that: 1) hepatitis A, B, and E have a strong seasonal
271 volatility, but hepatitis C fluctuates up and down monthly and does not have seasonal volatility;
272 and 2) the incidence data of hepatitis A and B are the smallest and the largest, respectively.
273 Hepatitis E increased slowly from January to December (except for March). That is to say,
274 these three prediction methods have their advantages when they are used to predict seasonal
275 fluctuation data. The BPNN-GA and WNN methods are suitable for predicting small and large
276 data, respectively, while GRNN is suitable for predicting data that increases steadily. The
277 BPNN-GA and WNN methods were not superior to the others when they were used to predict
278 the data that fluctuated up and down monthly and does not have seasonal volatility, and the
279 GRNN method is not suitable for predicting these types of data.

280 **Comparison of Statistical Significance Tests**

281 Statistical significance of the obtained results was investigated using T-test; a p-value
282 of <0.05 was considered significant. The results are listed in Table 3.

283 **Table 3** Comparison of Statistical Significance Tests in the prediction results.

284 (R is correlation coefficient)

285 The correlation will be better when the correlation coefficient is close to 1, namely, the
286 predicted value is closer to the observed value. From Table 3, it can be seen that the BPNN-GA
287 method has the best correlation when it was used to predict hepatitis B and C. The same in
288 regard to the GRNN and WNN method; they had the best correlation when they were used to
289 predict hepatitis E and A, respectively.

290 $P < 0.01$ are for all models from Table 3 which reveals that the difference is statistically
291 significant between the predictive value and the original data.

292 **Conclusion**

293 This research compared and evaluated the prediction of hepatitis by the BPNN-GA, GRNN,
294 and WNN methods. The prediction results will be affected by the data features. When the small
295 data set has seasonal fluctuation, the prediction result by BPNN-GA will be better than the two
296 other methods. The WNN method is suitable for predicting the large data set that has seasonal
297 fluctuation and the same for the GRNN method when the data increases steadily. The results of
298 all three methods show that the greater the disease fluctuations, the worse the prediction results.

299 The forecasting efficacies of three models are compared based on performances. GRNN is
300 learns faster and converges to the optimal regression surface. Capturing the dynamic behavior
301 of hepatitis incidence. Although the BPNN is easy to fall into the local optimum and has highly
302 non-linear weight update and slow coverage rate, the accuracy of forecasting could be improved
303 by optimizing the initial weights and thresholds. The advantage of the BPNN is that it is suited
304 for prediction the small data set has seasonal fluctuation. Compared to BPNN-GA and GRNN,
305 WNN has the best performance when it is used to predict large data set with seasonal
306 fluctuation.

307 This study can be extended in different directions. First, only hepatitis incidence is predicted

308 in the paper. In order to ascertain performance of three models and possible factors that will
309 impact on the model performance in practice, more infectious diseases should be considered.
310 Finally, we limited the analysis to only three ANN methods, and in future studies more methods
311 could be tested to predict incidence of important diseases, including hepatitis.

312 REFERENCE

- 313 1. **Available at:** <http://www.who.int>
- 314 2. **Eikenberry S, Hews S, Nagy JD, Kuang Y. 2009.** The dynamics of a delay model of HBV
315 infection with logistic hepatocyte growth. *Mathematical Biosciences and Engineering*,
316 **6(2):**283-99.
- 317 3. **Gourley SA, Kuang Y, Nagy JD. 2008.** Dynamics of a delay differential equation model of
318 hepatitis B virus infection. *Journal of Biological Dynamics*. **2(2):**140-153. DOI:
319 10.1080/17513750701769873.
- 320 4. **Chinese Society of Hepatology and Chinese Society of Infectious Diseases, Chinese**
321 **Medical Association.2010.** The guideline of prevention and treatment for chronic hepatitis
322 *B.Journal of Clinical Hepatology*: 2011-01.
- 323 5. **Zhang X, Liu Y, Yang M, Zhang T, Young AA, Li X. 2013.** Comparative Study of Four
324 Time Series Methods in Forecasting Typhoid Fever Incidence in China. *PLoS One* **8(5):**
325 e63116. DOI:10.1371/journal.pone.0063116.
- 326 6. **Zhang L, Zheng Y, Wang K. 2014.** An optimized Nash nonlinear grey Bernoulli model
327 based on particle swarm optimization and its application in prediction for the incidence of
328 Hepatitis B in Xinjiang, China. *Computers in Biology & Medicine*, **49C(1):**67-73. DOI:
329 10.1016/j.combiomed.2014.02.008.
- 330 7. **Ren H, Li J, Yuan ZA, Hu JY, Yu Y, Lu YH. 2013.** The development of a combined
331 mathematical model to forecast the incidence of hepatitis e in shanghai, china. *Bmc*

- 332 *Infectious Diseases*, **13(1)**:1-6. DOI: 0.1186/1471-2334-13-421.
- 333 8. **Ture M, Kurt I. 2006.** Comparison of four different time series methods to forecast hepatitis
334 A virus infection, *Expert systems with application*, **31(1)**:41-46. DOI:
335 10.1016/j.eswa.2005.09.002.
- 336 9. **Gan RJ, Chen XJ, Yan Y, Huang DZ. 2015.** Application of a hybrid method combining
337 grey model and back propagation artificial neural networks to forecast hepatitis b in China.
338 *Computational and Mathematical Methods in Medicine*, **Volume 2015**, Article ID 328273, 7
339 pages.<http://dx.doi.org/10.1155/2015/328273>.
- 340 10. **Thornley S, Bullen C, Roberts M. 2008.** Hepatitis b in a high prevalence new zealand
341 population: a mathematical model applied to infection control policy. *Journal of Theoretical*
342 *Biology*, **254(3)**:599-603. DOI: 10.1016/j.jtbi.2008.06.022.
- 343 11. **Weitschek E, Lo Presti A, Drovandi G, Felici G, Ciccozzi M, Ciotti M, Bertolazzi P.**
344 **2012.** Human polyomaviruses identification by logic mining techniques. *Virology journal*,
345 **9(1)**:1-6. DOI: 10.1186/1743-422X-9-58.
- 346 12. **Weitschek E, Cunial F, Felici G. 2015.** LAF: Logic Alignment Free and its application to
347 bacterial genomes classification. *Biodata Mining*, **8(1)**:39. DOI: 10.1186/s13040-015-0073-
348 1.eCollection 2015.
- 349 13. **Polychronopoulos D, Weitschek E, Dimitrieva S, Bucher P, Felici G, Almirantis Y.**
350 **2014.** Classification of selectively constrained DNA elements using feature vectors and rule-
351 based classifiers. *Elsevier Genomics*, **104(2)**:79-86. DOI: 10.1016/j.ygeno.2014.07.004.
- 352 14. **Tang Z.H, Liu J, Zeng F, Li Z, Yu X, Zhou, L. 2013.** Comparison of prediction model for
353 cardiovascular autonomic dysfunction using artificial neural network and logistic regression
354 analysis. *Plos One*, **8(8)**: e70571. DOI:10.1371/journal.pone. 0070571.
- 355 15. **Terrin N, Schmid CH, Griffith JL, D'Agostino RB, Selker HP. 2003.** External validity of

- 356 predictive models: a comparison of logistic regression, classification trees, and neural
357 networks. *Journal of Clinical Epidemiology*, **56(8)**:721-9. DOI:
358 10.1016/S0895-4356(03)00120-3
- 359 16. **Guan P, Huang DS, Zhou BS. 2005.** Forecasting model for the incidence of hepatitis a
360 based on artificial neural network. *World Journal of Gastroenterology*, **10(24)**:3579-82.
- 361 17. **Available at:** <http://www.phsciencedata.cn>
- 362 18. **Available at:** <http://www.gxws.gov.cn/cszc/jbkzc/yiqingxinxi>
- 363 19. **Ramesh BN, Arulmozhivarman, P. 2013.** Improving forecast accuracy of wind speed
364 using wavelet transform and neural networks. *Journal of Electrical Engineering &*
365 *Technology*, **8(3)**: 559-563. DOI: 10.5370/JEET.2013.8.3.559.
- 366 | 20. **Huang DZ, Gong RX, Gong S. 2015.** Prediction of wind power by chaos and bp artificial
367 | neural networks approach based on genetic algorithm. *Journal of Electrical Engineering*
368 &
369 *Technology*, **10(1)** : 41-46. DOI : 10.5370/JEET.2015.10.1.041.
- 370 21. **Mitchell, Melanie. 1996.** An Introduction to Genetic Algorithms. MA: MIT Press,
371 Cambridge, ISBN 9780585030944.
- 372 22. **Antonios K, Alexandridis, Achilleas D, Zapranis. 2014.** Wavelet Neural Networks: With
373 Applications in Financial Engineering, Chaos, and Classification. *John Wiley & Sons, New*
374 *Jersey, USA*, ISBN 9781118592526.
- 375 23. **Alexandridis AK, Zapranis AD. 2013.** Wavelet neural networks: a practical guide. *Neural*
376 *Network*. **42**:1-27. DOI: 10.1016/j.neunet.
- 377 | 24. **Specht D. 1991.** A general regression neural network. *IEEE Transactions on Neural*
378 *Networks*, **2(6)**:568-576. DOI: 10.1109/72.97934.
- 379 25. **Zhang Le, Suganthan PN. 2016.** A survey of randomized algorithms for training neural

- 380 networks. *Information Sciences*. **364**:146-155. DOI: 10.1016/j.ins.2016.01.039.
- 381 26. **Azadeh A, Ghaderi SF, Tarverdian S, Saberi M. 2007.** Integration of artificial neural
382 networks and genetic algorithm to predict electrical energy consumption. *Applied*
383 *Mathematic and Computation*. **186(2)**:1731-1741. DOI: 10.1016/j.amc.2006.08.093.

Figure 1 (on next page)

Figure 1 Topology structure of BPNN.

Figure 1

Input layer

Hidden layer

Output layer

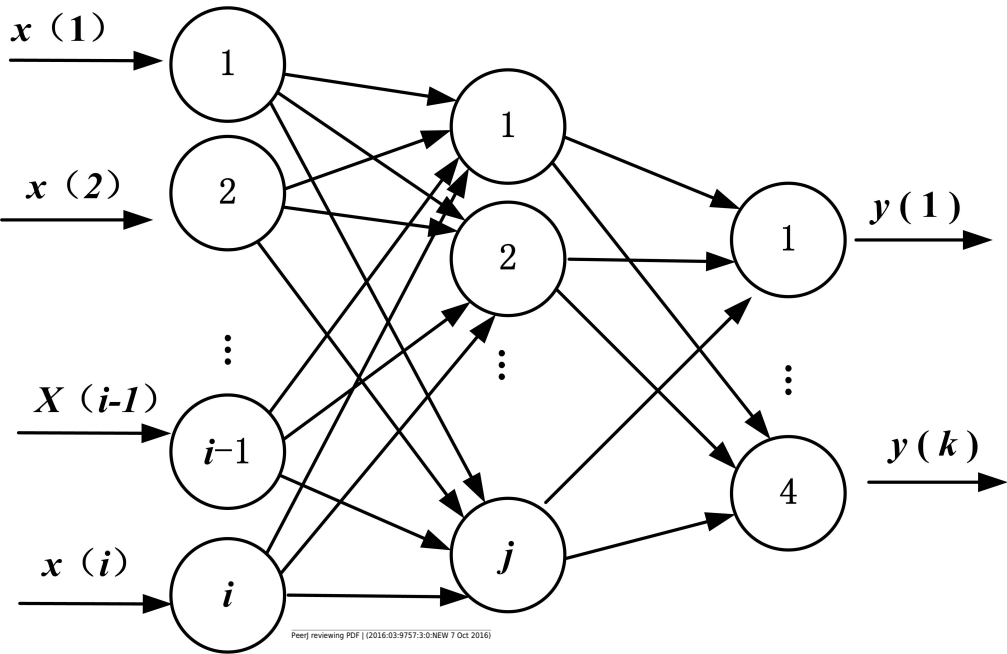


Figure 2 (on next page)

Figure 2 Flow chart of the BPNN prediction algorithm optimized by GA .

Figure 2

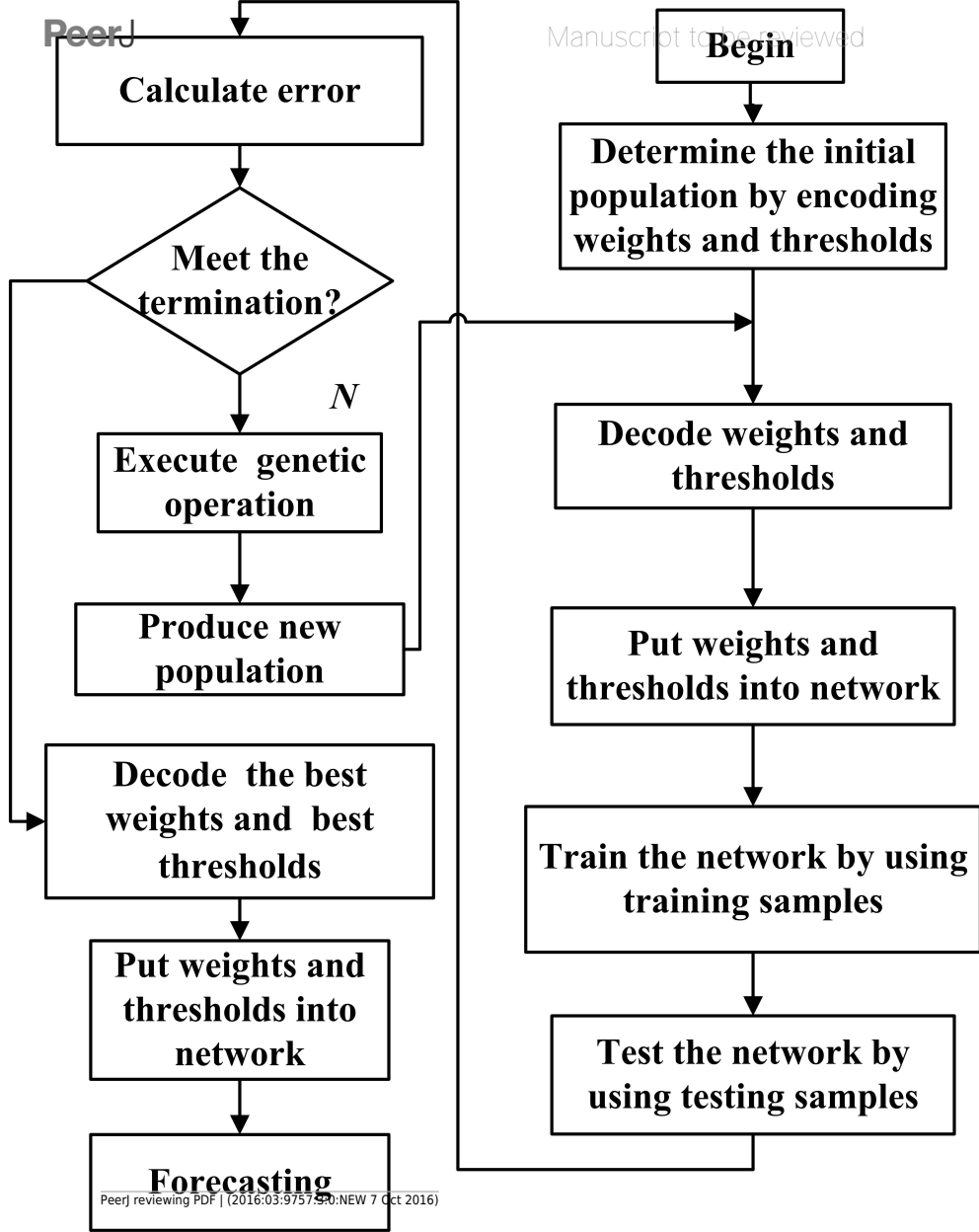


Figure 3 (on next page)

Figure 3 Topology structure of WNN.

Figure 3

PeerJ Manuscript to be reviewed

Input layer The Wavelet Basis Function Output layer

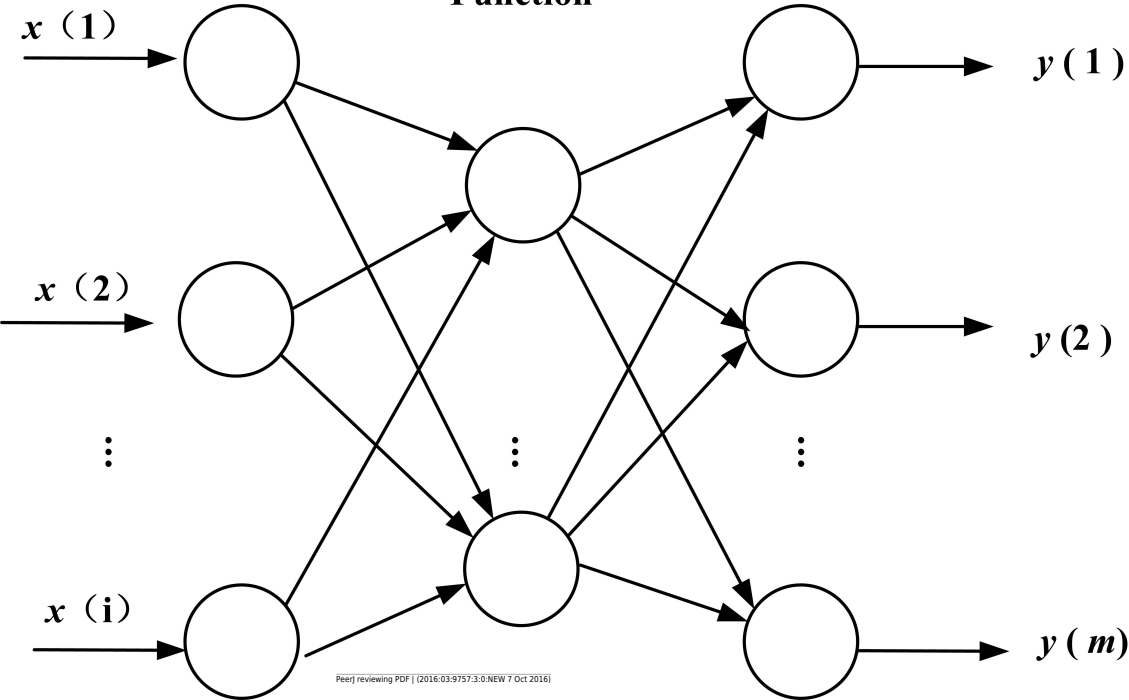


Figure 4 (on next page)

Figure 4 Flow chart of the WNN prediction algorithm.

Figure 4

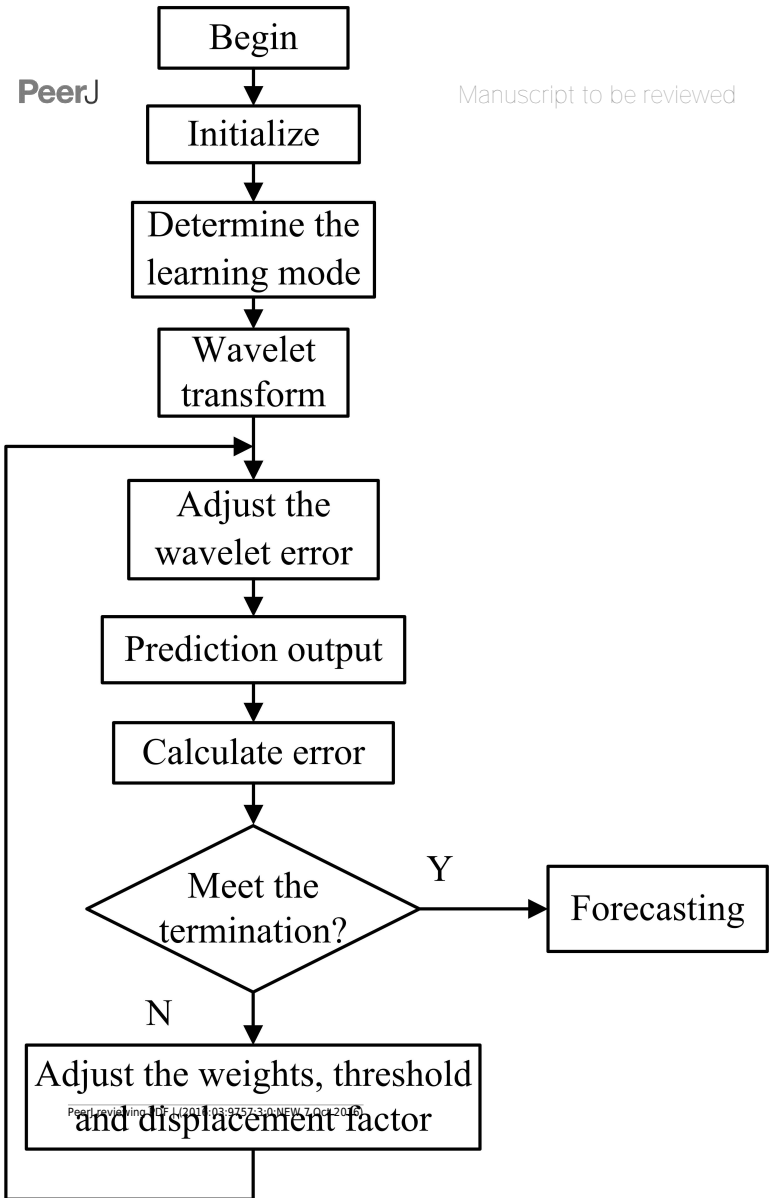


Figure 5 (on next page)

Figure 5 Topology structure of GRNN.

Figure 5

Input layer

Pattern layer

summation layer

Output layer

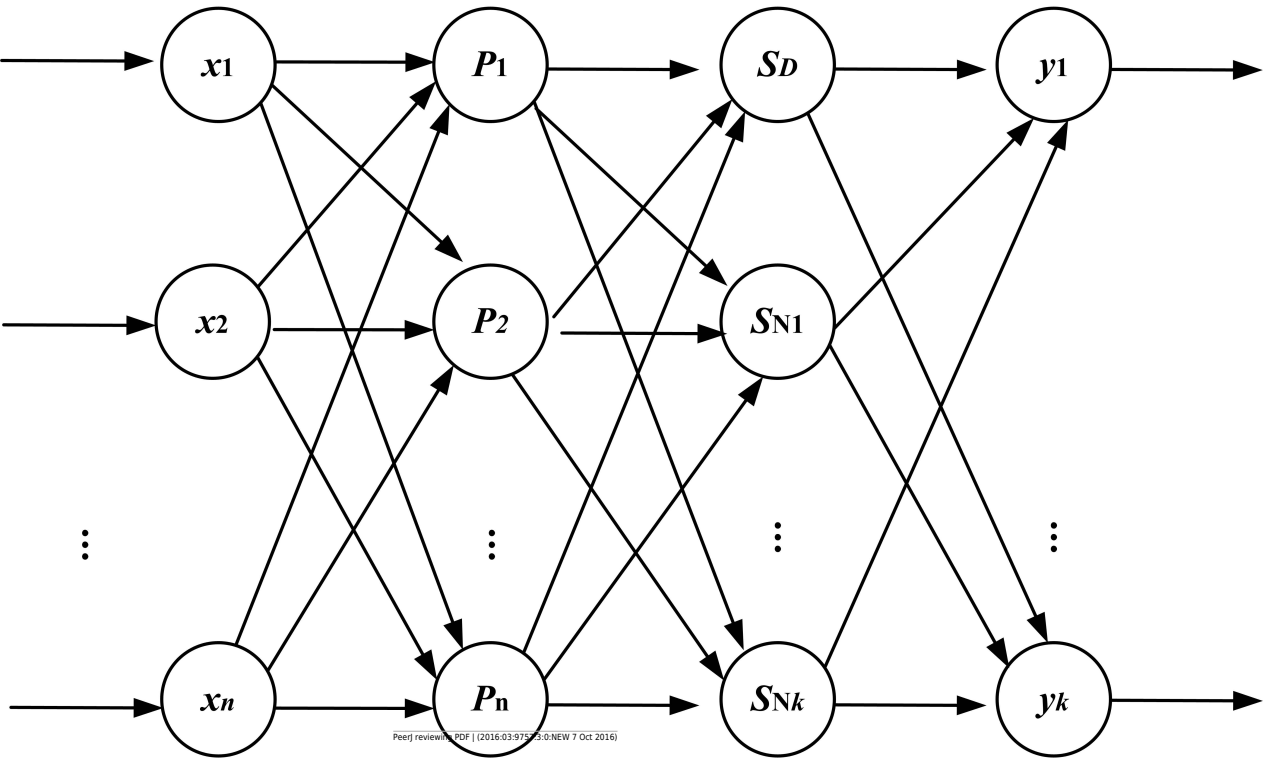


Figure 6 (on next page)

Figure 6 The main Incidence of hepatitis in Guangxi Province , China from January 2004 to December 2014.

Figure 6

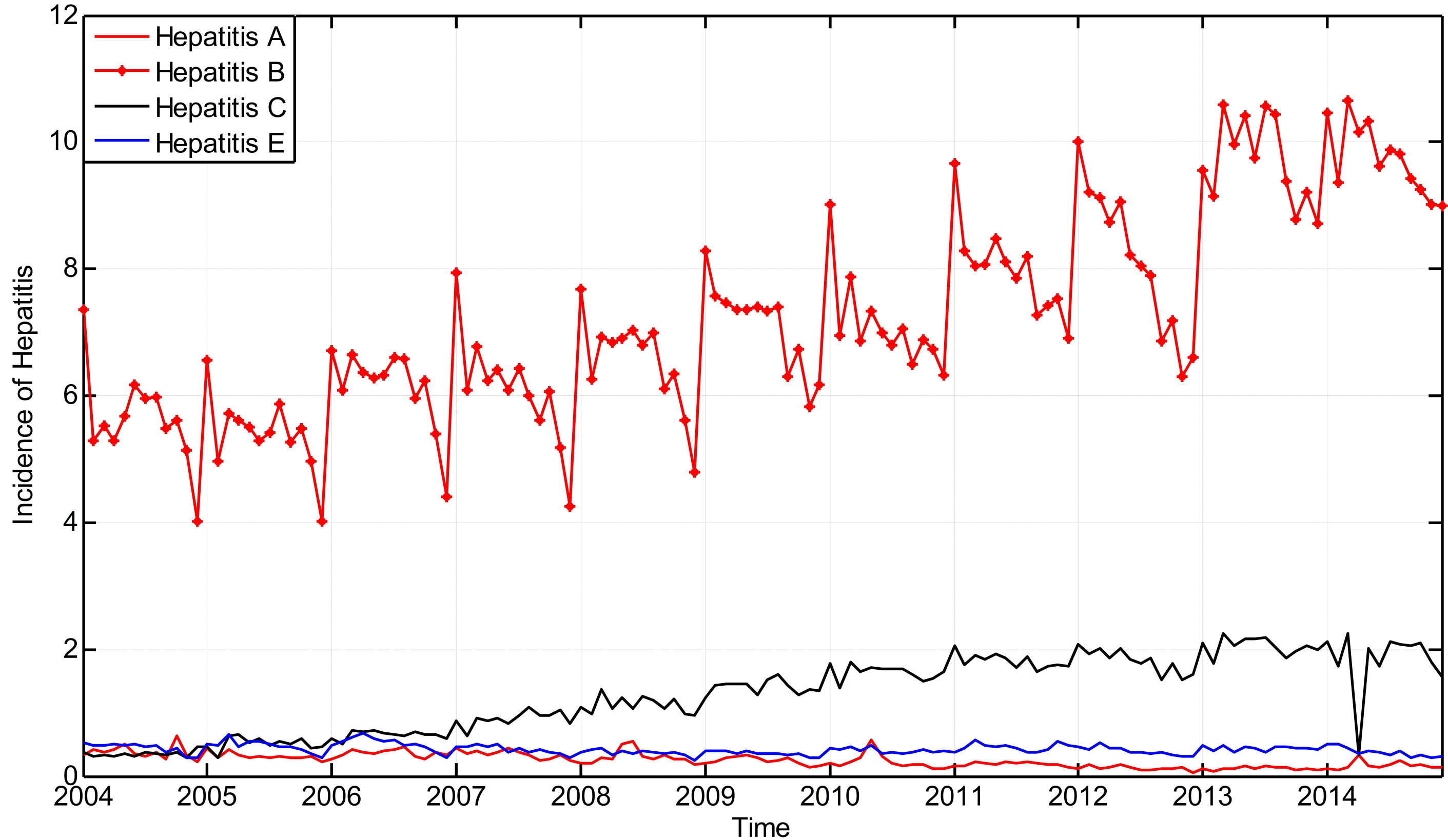
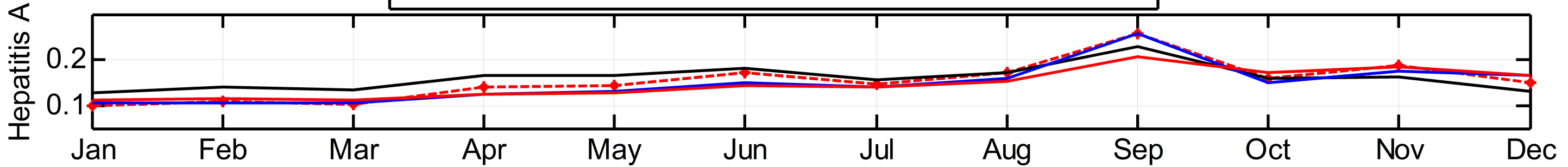


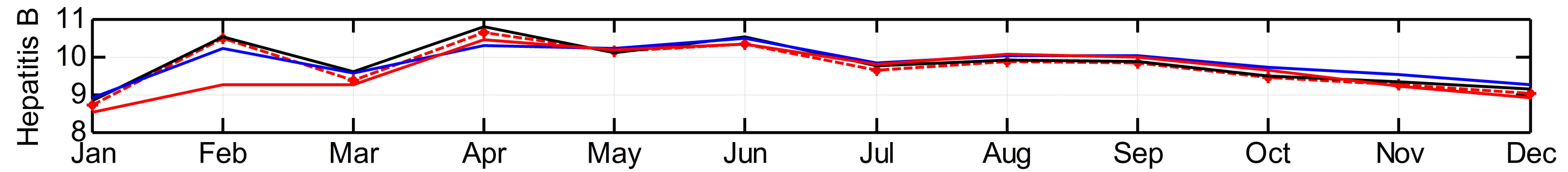
Figure 7 (on next page)

Figure 7 Contrast between observed values and predicted values using the three methods.

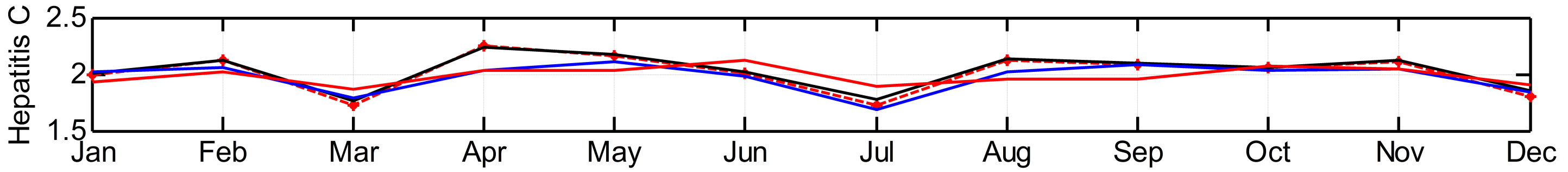
Figure 7



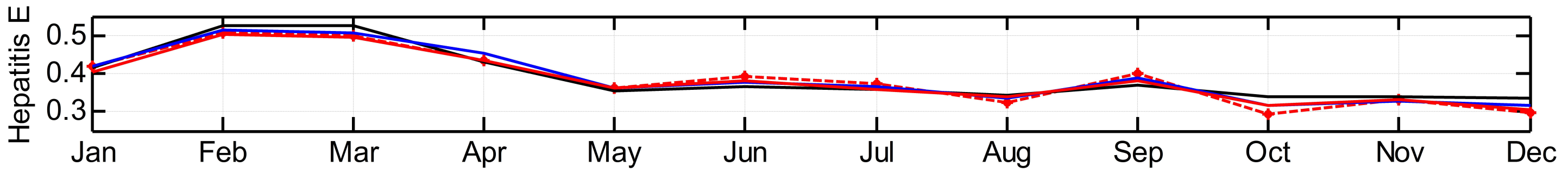
A



B



C

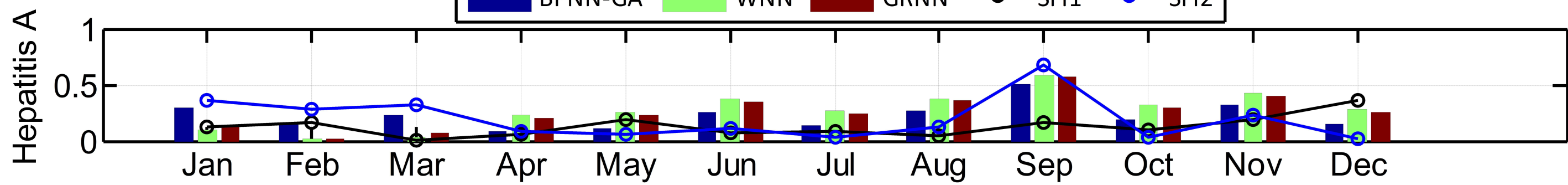


D

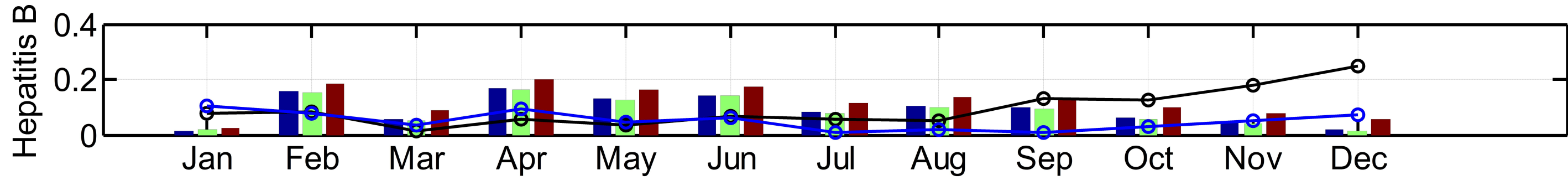
Figure 8(on next page)

Figure 8. The relationship between the seasonal fluctuation index and RE of the predictions by the three methods. (Histograms and curves represent RE of the predictions and the seasonal fluctuation index, respectively)

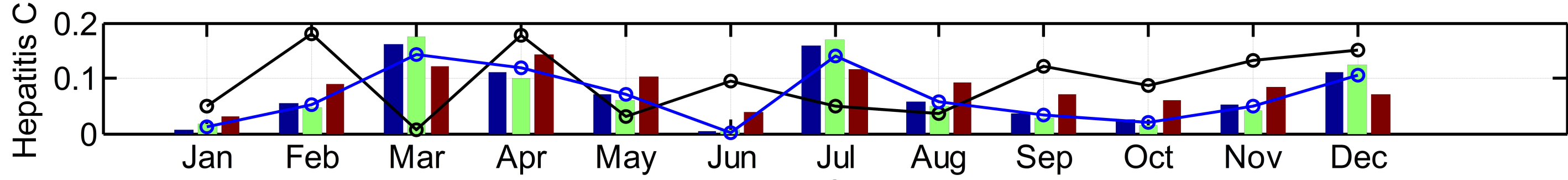
Figure 8



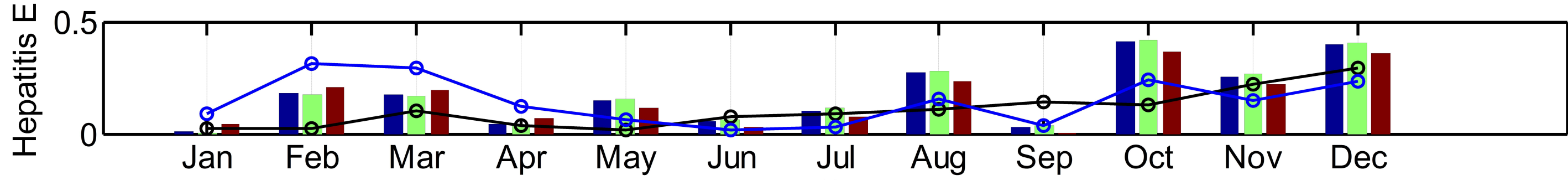
A



B



C



D

Table 1 (on next page)

Table 1 Parameters of the GA used to optimize the BPNN.

Table 1

1

Table 1 Parameters of GA

Population size	40
Algebra	50
Number of bits	10
Crossover probability	0.7
Mutation probability	0.01
Generation gap	0.95

2

Table 2 (on next page)

Table 2 Comparison of the evaluation indexes in the prediction results.(best performers are in bold fonts)

Table 2

1 **Table 2** Comparison of Evaluation Indexes (best performers are in bold fonts)

Hepatitis	Method	MSE	MAE	RMSE	SSE	MAPE
A	BPNN-GA	0.0024	0.0377	0.0488	0.0286	3.7743
	WNN	0.0038	0.0480	0.0616	0.0455	4.7955
	GRNN	0.0034	0.0456	0.0587	0.0413	4.5566
B	BPNN-GA	1.1018	0.9008	1.0497	13.2217	90.0830
	WNN	1.0285	0.8652	1.0141	12.3414	86.5163
	GRNN	1.7907	1.2085	1.3382	21.4889	120.8490
C	BPNN-GA	0.0273	0.1376	0.1651	0.3272	13.7552
	WNN	0.0273	0.1330	0.1652	0.3274	13.3042
	GRNN	0.0338	0.1713	0.1839	0.4058	17.1327
E	BPNN-GA	0.0054	0.0617	0.0733	0.0645	6.1665
	WNN	0.0055	0.0626	0.0745	0.0665	6.2620
	GRNN	0.0048	0.0577	0.0696	0.0582	5.7701

2

Table 3 (on next page)

Table 3 Comparison of Statistical Significance Tests in the prediction results. (R is correlation coefficient)

Table 3

1 **Table 3** Comparison of Statistical Significance Tests(R is correlation coefficient)

Hepatitis	Statistic value	BPNN-GA	WNN	GRNN
A	R	0.8992	0.9686	0.9129
	p-value	0.00006969	0.00000023	0.00003383
B	R	0.9916	0.9575	0.8030
	p-value	0.00000000	0.00000102	0.00166221
C	R	0.9991	0.9141	0.6903
	p-value	0.00000000	0.00003198	0.01295323
E	R	0.9409	0.9835	0.9847
	p-value	0.00000510	0.00000001	0.00000001

2